Compressive Properties of Mouse Articular Cartilage Determined in a Novel Micro-Indentation Test Method and Biphasic Finite Element Model

Li Cao
Department of Biomedical Engineering,
Duke University,
Box 90281, Durham, NC 27708

Inchan Youn
Division of Orthopaedic Surgery,
Department of Surgery,
Duke University Medical Center,
DUMC Box 3093,
Durham, NC 27710

Farshid Guilak

Lori A Setton
e-mail: setton@duke.edu

Department of Biomedical Engineering,
Duke University,
Box 90281,
Durham, NC 27708
and
Division of Orthopaedic Surgery,
Department of Surgery,
Duke University Medical Center,
DUMC Box 3093,
Durham, NC 27710

The mechanical properties of articular cartilage serve as important measures of tissue function or degeneration, and are known to change significantly with osteoarthritis. Interest in small animal and mouse models of osteoarthritis has increased as studies reveal the importance of genetic background in determining predisposition to osteoarthritis. While indentation testing provides a method of determining cartilage mechanical properties in situ, it has been of limited value in studying mouse joints due to the relatively small size of the joint and thickness of the cartilage layer. In this study, we developed a micro-indentation testing system to determine the compressive and biphasic mechanical properties of cartilage in the small joints of the mouse. A nonlinear optimization program employing a genetic algorithm for parameter estimation, combined with a biphasic finite element model of the micro-indentation test, was developed to obtain the biphasic, compressive material properties of articular cartilage. The creep response and material properties of lateral tibial plateau cartilage were obtained for wild-type mouse knee joints, by the micro-indentation testing and optimization algorithm. The newly developed genetic algorithm was found to be efficient and accurate when used with the finite element simulations for nonlinear optimization to the experimental creep data. The biphasic mechanical properties of mouse cartilage in compression (average values: Young's modulus, 2.0 MPa*; Poisson's ratio, 0.20; and hydraulic permeability,* 1.1×10^{-16} $m^4/N\text{-}s$*) were found to be of similar orders of magnitude as previous findings for other animal cartilages, including human, bovine, rat, and rabbit and demonstrate the utility of the new test methods. This study provides the first available data for biphasic compressive properties in mouse cartilage and suggests a promising method for detecting altered cartilage mechanics in small animal models of osteoarthritis.*
[DOI: 10.1115/1.2246237]

Keywords: mechanical properties, indentation, compression, cartilage, biphasic, finite element model, optimization, genetic algorithm, mouse, osteoarthritis

1 Introduction

Articular cartilage serves as the load-bearing tissue that lines the ends of bones in diarthrodial joint. The unique mechanical properties of articular cartilage serve as important measures of tissue function, damage, or degeneration. With joint degenerative diseases such as osteoarthritis (OA), the compressive, tensile, and shear moduli of articular cartilage are reduced [1–4], and similar changes are evident in instability models of OA [5–9]. In addition, the hydraulic permeability, a measure of the intrinsic flow-dependent properties of cartilage, is elevated in cartilage from OA joints [2,5,6]. The reduced compressive stiffness and elevated permeability in these tissues have been attributed to increased water content and associated decreases in proteoglycan content that reduce the fluid-pressurization mechanism of load support. Many of these changes in cartilage mechanics have been correlated with histological and gross evidence of cartilage damage and collectively point toward a diminished ability to provide load support and distribution during joint loading, in a process that may contribute to progressive joint disease.

In recent years, significant interest has turned toward mouse models of OA that provide the ability to test the role of genetic background on the progression of osteoarthritis [10]. The determination of cartilage mechanical properties in small animal joints is challenging, however, due to difficulties with handling specimens, resolving low forces, and resolving the very small deformations of cartilage with layer thicknesses less than 500 μm. In our prior work, we have developed an osmotic swelling test that was used to examine changes in the tensile modulus of knee joint cartilage with spontaneous OA during natural aging in the guinea pig [11], or in a type XI collagen insufficiency model in the mouse [12]. However, this method cannot be used to measure the compressive properties of cartilage, which may provide further insight into the role of specific matrix macromolecules in determining cartilage function.

Athanasiou and co-workers have reported the compressive modulus and hydraulic permeability of rat knee cartilage obtained with a modified indentation test and nonlinear optimization to a biphasic finite element model [13]. Results showed that diet restriction had no effects on the compressive biomechanical properties of articular cartilage, while modest aging effects were found at 6 and 12 months of age. The compressive behavior of mouse humeral cartilage has also been studied in an indentation testing configuration using a comparatively large indenter (diameter

Contributed by the Bioengineering Division of ASME for publication in the JOURNAL OF BIOMECHANICAL ENGINEERING. Manuscript received August 30, 2005; final manuscript received April 19, 2006. Review conducted by Yoram Lanir.

350 μm), to analyze changes in cartilage mechanics in mice heterozygous for a type II collagen gene knockout (*Col2a1* +/−, [14]). In that study, the indentation stiffness was reported, rather than intrinsic material properties, because of recognized limitations in quantifying modulus or permeability from an appropriate model of an indentation test. A combined micro-indentation testing system that is appropriately sized for the mouse cartilage and concordant with an appropriate theoretical model of transient behaviors will be important for quantifying intrinsic biphasic compressive properties of cartilage in the very small joints of the mouse knee.

To extract material properties from experimental data, an efficient global optimization algorithm for parameter estimation is needed for nonlinear numerical analysis. When the objective function with a dependence on multiple variables is nonlinear and not differentiable by analytical methods, direct search approaches provide a computationally advantageous alternative. Two commonly used direct search algorithms are the Nelder-Mead simplex method (NM) [15] and genetic algorithm (GA) [16], used here. The GA starts with a set of random solutions called a "population." In reference to biological theories of evolution, the "fitness" of solutions within a population will be evaluated and those members with better fitness will have more chance to "reproduce," or "replicate" themselves under mathematically specified crossover and mutation rules. The new "offspring" with better fitness will then form a new population. In this manner, the concept of GA is mathematically evoked until the best fit is found. Compared to NM, GA is inherently parallel and may be better able to escape local minima and find global minimum, although not tested here. To reduce computational cost of the GA and obtain better convergence performance, the characteristics of the objective function dependence on the target parameters and implementation with the FEM code need to be carefully examined and developed.

The objective of our study was to develop a micro-indentation system with geometries and force analyses appropriate for the study of cartilage in mouse joints. A secondary objective was to develop a numerical optimization scheme combined with a biphasic finite element model (FEM) that was efficient and precise for use with large scale computational analyses. We developed custom instrumentation in combination with a commercially available materials testing system to measure the viscoelastic creep behaviors of mouse articular cartilage. A computational genetic algorithm was also developed to interface with a linear biphasic FEM and a nonlinear cost function to determine the three independent biphasic material parameters of cartilage, including compressive modulus, Poisson's ratio, and hydraulic permeability. The method was applied to quantify cartilage mechanics on the lateral tibial plateau of C57BL/6 or "wild-type" mice to demonstrate proof-of-concept for the newly developed methods.

2 Materials and Methods

Specimen Preparation. Mouse knee joints were obtained from 6-month-old C57BL/6 mice which were bred and raised under Harvard's Institutional Care and Use Committee. Knee joints (n =6, 2 right and 4 left limbs from 4 animals) were harvested and tibiae were dissected and stored at −20°C until testing. Right before testing, menisci were carefully removed from the tibial cartilage surface under a stereomicroscope and a notch made on the lateral-most edge of the tibial surface which served as a landmark for the coronal site of tissue testing (Fig. 1). The tibial bone shaft was embedded in epoxy putty (EP-400, Rectorseal Co., Houston, TX) to expose the tibial plateau, mounted in the specimen chamber, and immersed in phosphate buffered saline (PBS) at room temperature.

Micro-indentation Testing. An electromechanical test system and associated software (ELF 3200 and Wintest®, EnduraTEC, Minnetonka, MN) were used for these studies. The test system was instrumented with a low capacity load-cell (50 g, resolution

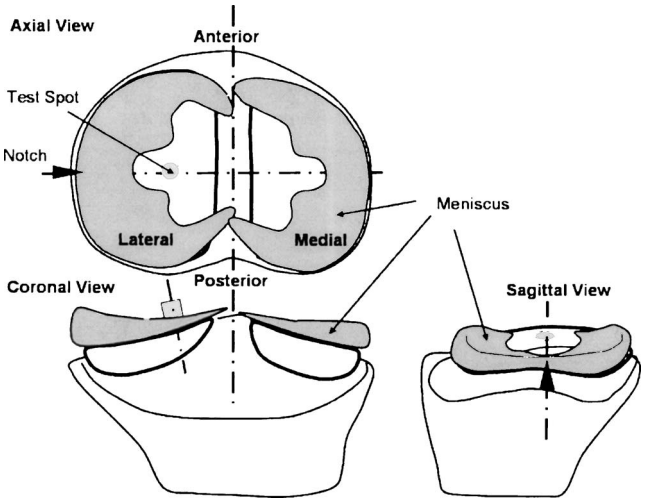

Fig. 1 Schematic of specimen preparation. The testing spot was in the cartilage-cartilage contact area uncovered by meniscus on the lateral tibial plateau. The notch was made from top view under a stereomicroscope. The indenting site was decided by both posterior view and lateral view through a digital camera system.

0.01 g, accuracy 0.05 g, Sensotec, Columbus, OH) and an extensometer (1 mm, resolution 0.1 μm, accuracy 0.5 μm, Epsilon, Jackson, WY) to measure load and displacement, respectively (Fig. 2). Micro-scale, plane-ended indenters were machined from glass fibers (∅:110 μm, longitudinal modulus ~40 GPa, Thorlabs, Newton, NJ) by a high precision fiber cleaver (CT-04B, Fujikura Ltd., Kumamoto, Japan). The specimen position was adjusted by a custom-built universal joint (5 DOF) constructed from three precision linear stagers (x, y, and z direction) and a double angle goniometer (±15°, Thorlabs, Newton, NJ). Due to the natural curvature of the articular surface, a dual-angle camera system was used to optically confirm that the indenter tip was perpendicular to the cartilage surface by the user (Fig. 3).

All indentation creep testing was performed at the lateral tibial plateau site. A preload (0.15 g) was applied under the force feedback control mode to ensure contact at the cartilage-indenter interface. Transient deformation of the cartilage surface was moni-

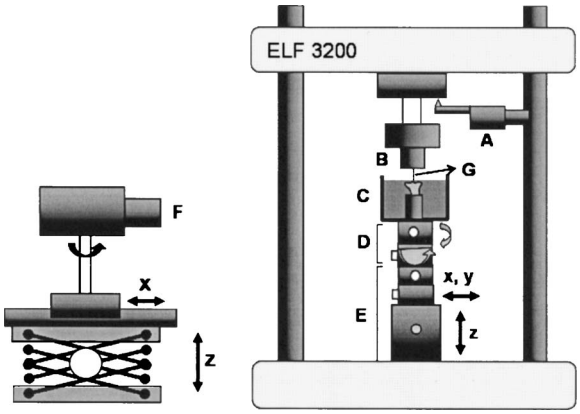

Fig. 2 Schematic of micro-indentation testing system (A: Extensometer; B: Load Cell; C: Specimen Chamber; D: Goniometers; E: Linear Stagers; F: Digital Camera; G: Glass Fiber Indenter). The double angle goniometer and three linear stagers under the specimen chamber allow five DOF of position control of the specimen. A digital camera system captures images from two different angles, assuring the normal surface contact between the indenter and cartilage surface.

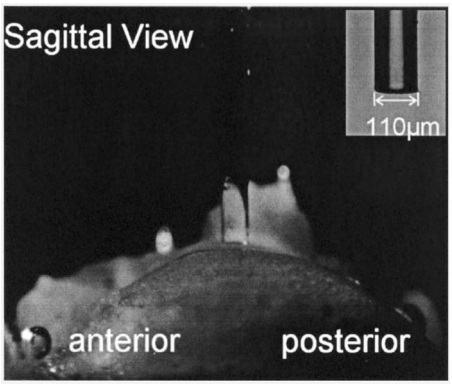

Fig. 3 Lateral view of a flat-ended glass fiber indenter on lateral tibial plateau. An indenter with a smaller diameter gives better surface contact, especially for highly curvy cartilage surface in mouse knee joints.

tored by the extensometer. After equilibration of the tare load for ~300 s, a test load was applied in a nearly step-wise manner (0.2 g, 500 g/s) and displacement of the cartilage surface was recorded at a sampling rate of 1 Hz. Preliminary work confirmed that equilibrium displacement of the cartilage surface was generally achieved within 100 s under this load, so that displacement data were recorded to twice this value or 200 s to allow for variability in incorporation of equilibrium deformation across all samples.

Histology and Cartilage Thickness Measurement. After mechanical tests, the specimens were fixed in buffered neutral 10% formalin (#3190-1, Ricca Chemical) overnight, decalcified (CalEX, Fisher Scientific) for 36 h, dehydrated through graded ethyl alcohol, and then embedded in paraffin. Successive 5-μm-thick sections were cut with a rotary microtome through the tissue block in the vicinity of the lateral landmark notch. After deparaffining in xylene and rehydration in graded alcohols, tissue sections were processed with safranin-O and fast green counter-staining and images viewed under light microscopy. The average tissue thickness from cartilage surface to tidemark was measured from six linear projections per section from the tidemark to cartilage surface on three consecutive sections with evidence of the lateral landmark notch (Fig. 4). Semiquantitative grading of cartilage histological appearance was also performed using a modified Mankin score [17] with four subcategories including cartilage structure, chondrocytes, tidemark integrity and Safranin-O staining (score range: 0–14, 0=normal cartilage, 14=extensively degenerated).

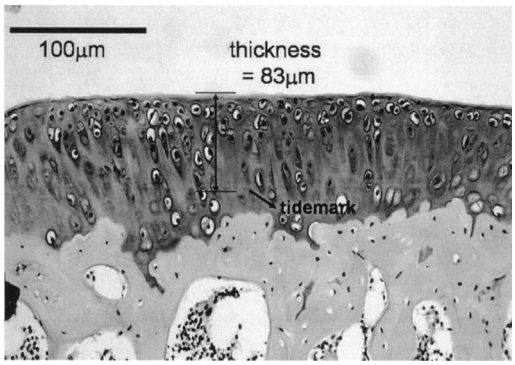

Fig. 4 Photomicrograph of mouse cartilage section stained with Safranin-O/Fast Green. Estimate of thickness measurement is shown.

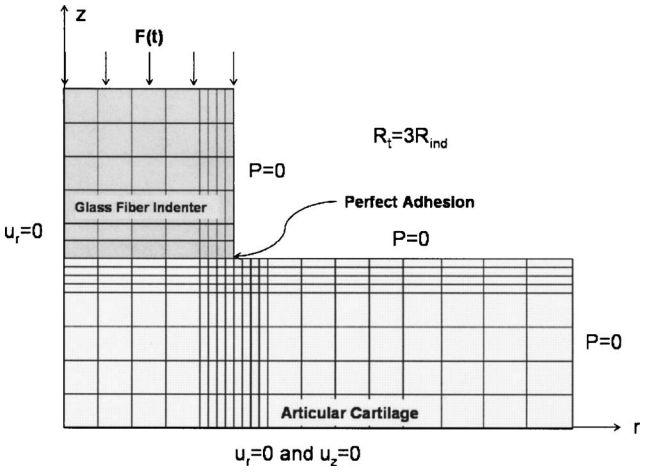

Fig. 5 Finite element mesh and boundary condition (*u-p* formulation) for an axisymmetric micro-indentation configuration. The indenter height is the same as cartilage thickness. The meshed cartilage region is three times the size of glass fiber indenter. R_t and R_{ind} are the radii of meshed cartilage and the indenter, respectively. $F(t)$ is the applied constant force. u_r and u_z are radial displacement and axial displacement, respectively, and p is the pressure.

Optimization Using Finite Element Model (FEM) and Differential Evolution (DE). Simulation of the biphasic indentation creep test was performed using a custom-written program based on an axisymmetric, linear and biphasic FEM [18] of the microindentation test (Fig. 5). Articular cartilage was modeled as an isotropic and linearly elastic biphasic material [19] with a dependence on Young's modulus E_s, Poisson's ratio ν_s, and constant permeability k. The cartilage layer was modeled upon a rigid and impermeable substrate, and the indenter was modeled as rigid and impermeable. Perfect adhesion was assumed for the interface of the cartilage and indenter. Preliminary tests of convergence were performed to determine the optimal radial dimension for the cartilage layer over the range $R_t/R_{ind}=2$ to 4, and to determine the appropriate mesh size over the range of 55 to 528 elements. Convergence was observed for all cases, and repeatable optimization results were also achieved for all sample radii and for mesh sizes greater than 156 elements. Thus, cartilage with the radius of three times of the indenter ($R_t/R_{ind}=3$) was meshed, and a total of 208 quadrilateral elements (160 for cartilage and 48 for the indenter) were used for all optimizations performed in this study.

In order to numerically match the FEM simulations to the experimental creep data to extract material properties, a differential evolution (DE) algorithm [20] was coupled with FEM for nonlinear optimization. DE is a population based, stochastic function minimizer which has been used in multiple objective optimizations [21]. Similar to other genetic algorithms, the concept behind DE is mathematically defined by the scheme for generating trial parameter vectors (offsprings). An initial population of trial vectors is generated randomly with a uniform distribution over the parameter space, and objective functions are calculated for each trial vector in the population. In successive iterations (generations), three parameter vectors from the previous iteration are randomly selected and new trial vectors are generated from these vector differences and a scaling factor. By using vector differences for perturbing the vector population, no separate probability distribution for choosing trial parameter vectors has to be used, which makes the scheme completely self-organizing. In the new population of trial vectors, objective function calculations are repeated, and the vector with less cost (lower value of the objective function) survives in this population. This process is repeated until established convergence criteria are satisfied. In comparison to other optimization methods, DE provides one of the more robust

genetic algorithms for solving real-valued test function sets [22].

In this study, the objective function was defined as the sum of squared errors between experimental data and FEM simulation as $U=\Sigma_{i=1}^{nt}(u_i-\hat{u}_i)^2$, where nt is the total sampling points (100) over sampling time (100 s), and u and $\hat{u}$ are creep displacements from indentation experimental measurements and computational simulations, respectively. The DE algorithm required definitions of five controlling system variables as inputs, including the strategy and scaling factor to generate trial vectors, number of populations, crossover ratio, and the maximum iterations allowable for convergent results. In the parametric study of FEM/DE program, different combinations of five controlling variables were tested and an optimal combination was chosen for all optimizations for better convergence. The parameter vector of the FEM/DE optimization program was comprised from the biphasic material parameters (E_s, ν_s, k) for the linear elastic model. The ranges examined were $E_s=[1.0, 2.5]$ MPa, $\nu_s=[0.1, 0.4]$, and $k=[1\times10^{-17}, 1\times10^{-14}]$m^4/N·s, respectively. Iterations within this parameter space were driven until the FEM/DE optimization yielded globally converged material parameter vectors for each specimen. The computational cost depended on the choice of the size of population and total iterations needed, which controlled how many times the objective function was called. Goodness of fit was evaluated by both residuals and root mean square errors (RMSE). Based on preliminary data, when RMSE is less than 3×10^{-7} and the residual is less than 3×10^{-6}, the optimization was considered convergent.

To test the sensitivity of the FEM/DE optimization program to initial populations, a calibration creep curve was generated by FEM with known material parameters. The FEM/DE optimization was repeated with seven different sets of initial populations. Errors between the optimized parameters and known target parameters were calculated. Since thickness was a critical measurement in very thin mouse cartilage, the effect of thickness measurement error on parameters determined from optimization was also evaluated. The random error in one single thickness measurement was ±5% due to variations in cartilage layer morphology and tissue sectioning. The main source of error was assumed to be systematic error due to tissue shrinkage during the histological fixation process [23]. While no independent method of thickness measurement was used here, due to complexities in handling mouse cartilage, preliminary work with other cartilages suggested that the "upper" limit of the systematic error was estimated to be −15%. Propagation of this measurement error into determination of optimized parameters was performed by varying cartilage thickness values by −20% to +5% of the baseline value (experimental measurement) and reporting the range of parameter outputs as estimates of parametric uncertainty.

3 Results

Histomorphometric Parameters. Cartilage layer thicknesses and histological grade were measured for lateral testing sites. The thickness was 82±9 μm (mean ±SD, $n=6$). Overall, there was little histological evidence of cartilage degeneration in the wild-type mouse knee joints at 6 months of age, with mean Mankin scores of 1.0 (SD:±0.6) as compared to 0 for nondegenerate cartilage.

Performance of the FEM/DE Optimization. In the sensitivity test, the average error between target and estimated parameters was less than 5% of calibration values for each parameter (Fig. 6). The elastic modulus and Poisson's ratio showed no sensitivity to different initial populations while permeability showed some small variation. The thickness measurement error contributed to little variability in estimation of the Poisson's ratio (Fig. 7), but contributed more error (less than 30%) to the permeability estimates. Optimized values for the compressive modulus increased with increasing values for thickness as expected, with a parameter estimation error less than 20%.

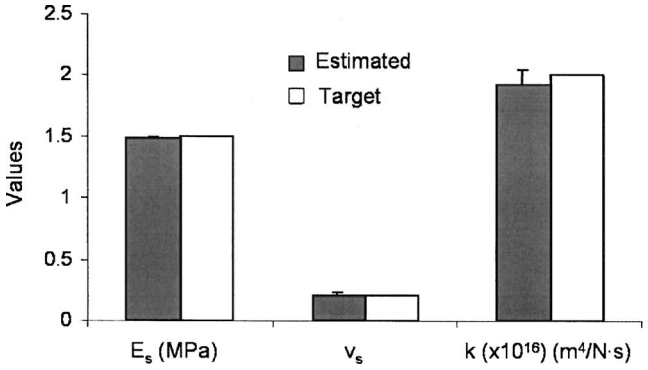

Fig. 6 Sensitivity test of optimization. Known target parameters are used to generate calibration creep data by FEM. Estimated parameters are optimized for the calibration data with different initial populations (n=7).

Mouse Cartilage Properties. Cartilage of the tibial plateau showed typical creep behavior, characterized by a jump in displacement from the step load, followed by increased deformation until equilibrium at ~75 s (Fig. 8). Displacement varied by less than 1% after 100 s. In the optimization of mouse cartilage, solutions generally converged to a parameter set within 20 iterations, for the chosen mesh and control variables. Values (mean ±SD, $n=6$) for the compressive modulus, Poisson's ratio, and hydraulic permeability were found to be 2.0±0.3 MPa, 0.20±0.03, and $1.1\pm0.4\times10^{-16}$ m^4/N-s, respectively, for the lateral tibial plateau cartilage. The average root mean square error for all optimizations was $1.81\pm0.52\times10^{-7}$.

4 Discussion

This study demonstrates that biphasic material properties of cartilage in a small animal, such as mouse, can be obtained using

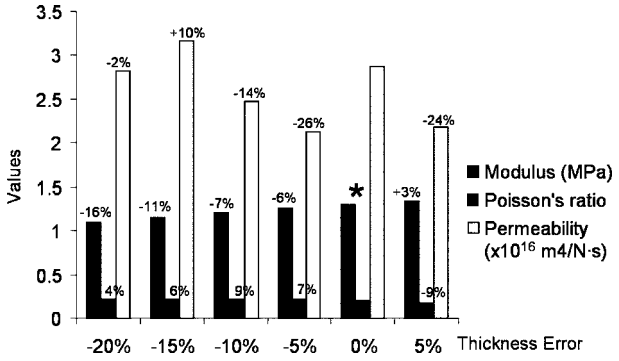

Fig. 7 Effects of thickness measurement errors on parameter estimates. Measurement errors on the order of 0–20% of average thickness values were incorporated in the optimization of the model to experimental data to estimate an uncertainty in parameter values. Parameters are shown for optimized values of *Es* and *k* against the introduced variation in measurement plotted on the *x* axis. The deviation in the parameter estimate from the "true" value is given at the top of each bar, to illustrate the range of parameter values as an estimate of the uncertainty. Overall, the error associated with variability in parameter estimation is less than the corresponding thickness measurement error. Note that values for the Poisson ratio varied by less than 10% in all optimization procedures. An asterisk indicates the baseline case in which the "true" thickness was used for optimization.

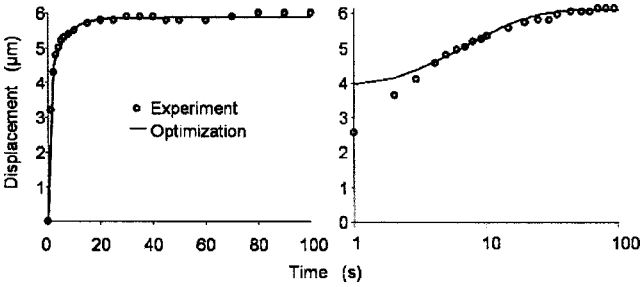

Fig. 8 A typical creep response on both linear (left) and logarithm (right) scales for the lateral tibial plateau uncovered by meniscus with a corresponding curve fit from the optimization

a micro-indentation testing system and a FEM/DE optimization algorithm. The intrinsic compressive properties of mouse cartilage measured here are of similar orders of magnitude to those previously for human and other animal articular cartilages [13,24–29]. Average values of ~0.7 MPa and ~1.2 MPa reported for the Young's modulus of rat femoral condylar [13] and human femoral head cartilage [25] are only slightly lower than values of ~2.0 MPa for the mouse cartilage reported here. Similarly, values for the permeability of mouse cartilage of $\sim 0.11 \times 10^{-15}$ m^4/N-s are lower but of a similar order of magnitude of reported values for the rat and human cartilage (0.9 and 3.1 $\times 10^{-15}$ m^4/N-s, respectively). Finally, the value for the Poisson's ratio of 0.2 obtained in this study for mouse cartilage is similar to that of the rat (0.21, [13]). It is noteworthy that values for the Young's modulus of mouse cartilage obtained from indentation testing are lower than that obtained by quantitating cartilage swelling (~4 MPa [12]), a difference that is at least partly attributable to differences in cartilage behaviors in compression and tension [30].

The DE algorithm used in this study was chosen to reduce the computational cost and complexity of performing nonlinear optimization with FEM simulations. It was shown to be accurate and repeatable in the sensitivity test. It avoids a need for gradient calculation and line search, which usually cause singularity problems and high cost in a typical FEM/optimization. In this program, the optimized solution may not be unique in the parameter space, but it generally converged within 20 iterations. The other advantage of this algorithm is that the optimization is not sensitive to the initial population. Thus, a "good" guess is not necessary for the first iteration in the application of the FEM/DE routines, only specification of bounds for each parameter is necessary that were rather large, e.g., Poisson's ratio: 0.1 to 0.4. However, in other FEM optimizations, a "bad" guess may cause divergence and sometimes extra effort, such as a semi-analytical or semi-numerical procedure that is needed to obtain a "good" initial estimate before applying the FEM/optimization routine [13]. While genetic algorithms such as DE have been widely used as a robust tool for optimal design and neural network learning, this study represents a new application of this technique for determining mechanical properties via an "inverse" FEM method.

One of the main difficulties involved in mechanical testing of mouse cartilage is the small size of the joint and the associated small and variable cartilage thickness. The cartilage layer of ~80 μm was very thin in comparison to other animals, such as the humeral head of mice (~120 μm, [14]) and rat (~150 μm, [13]), femoral condyles of rabbit (~250 μm), monkey (~570 μm), dog (~580 μm), and bovine (~940 μm, [23]). Furthermore, variability in the cartilage thickness due to "waviness" of the tidemark interface with the cartilage layer represent a greater percentage of the total cartilage layer. Satisfying the constraint of a low aspect ratio (indenter radius: cartilage thickness) and zero surface curvature for the indentation test become the limiting factors for testing such small animal joints. The small indenter made of glass fiber (~100 μm) was chosen to match the cartilage thickness in our mouse model, yet has a large enough surface to provide a measurable force response with low noise. With these limitations, the testing of thinner or more highly curved cartilage layers, such as those in the femoral condyle or femoral head, may require an even smaller indenter and higher resolution load cells and extensometers.

Given the complexity of evaluating cartilage thickness in small animal joints, the systematic error in the thickness measurement was considered as the main source of experimental error. The total error in accuracy due to the histological thickness measurement method could be as high as 20%, which were associated with an estimated uncertainty in parameters of the same order (<20% of parametric values)

In summary, this study demonstrates the use of a newly developed micro-indentation testing system and a FEM/DE optimization algorithm for studying cartilage mechanics in small animal joints. This study provides data for the biphasic compressive material properties in mouse cartilage and suggests a promising method for detecting biomechanical changes in small animal models of OA.

Acknowledgment

The authors would like to thank Dr. Mansoor Haider for help of the optimization algorithm. This study was supported by NIH Grant Nos. AR45644, AR50245, EB02263, AG15768, and AR39740.

References

[1] Akizuki, S., Mow, V. C., Muller, F., Pita, J. C., Howell, D. S., and Manicourt, D. H., 1986, "Tensile Properties of Human Knee Joint Cartilage. I. Influence of Ionic Conditions, Weight Bearing, and Fibrillation on the Tensile Modulus," J. Orthop. Res., **4**(4), pp. 379–392.

[2] Armstrong, C. G., and Mow, V. C., 1982, "Variations in the Intrinsic Mechanical Properties of Human Articular Cartilage With Age, Degeneration, and Water Content," J. Bone Jt. Surg., Am. Vol., **64**(1), pp. 88–94.

[3] Kempson, G. E., 1991, "Age-Related Changes in the Tensile Properties of Human Articular Cartilage: A Comparative Study Between the Femoral Head of the Hip Joint and the Talus of the Ankle Joint," Biochim. Biophys. Acta, **1075**(3), pp. 223–230.

[4] Roberts, S., Weightman, B., Urban, J., and Chappell, D., 1986, "Mechanical and Biochemical Properties of Human Articular Cartilage in Osteoarthritic Femoral Heads and in Autopsy Specimens," J. Bone Joint Surg. Br., **68**(2), pp. 278–288.

[5] Elliott, D. M., Guilak, F., Vail, T. P., Wang, J. Y., and Setton, L. A., 1999, "Tensile Properties of Articular Cartilage Are Altered by Meniscectomy in a Canine Model of Osteoarthritis," J. Orthop. Res., **17**(4), pp. 503–508.

[6] Setton, L. A., Mow, V. C., Muller, F. J., Pita, J. C., and Howell, D. S., 1994, "Mechanical Properties of Canine Articular Cartilage Are Significantly Altered Following Transection of the Anterior Cruciate Ligament," J. Orthop. Res., **12**(4), pp. 451–463.

[7] Guilak, F., Ratcliffe, A., Lane, N., Rosenwasser, M. P., and Mow, V. C., 1994, "Mechanical and Biochemical Changes in the Superficial Zone of Articular Cartilage in Canine Experimental Osteoarthritis," J. Orthop. Res., **12**(4), pp. 474–484.

[8] Sah, R. L., Yang, A. S., Chen, A. C., Hant, J. J., Halili, R. B., Yoshioka, M., Amiel, D., and Coutts, R. D., 1997, "Physical Properties of Rabbit Articular Cartilage After Transection of the Anterior Cruciate Ligament," J. Orthop. Res., **15**(2), pp. 197–203.

[9] LeRoux, M. A., Arokoski, J., Vail, T. P., Guilak, F., Hyttinen, M. M., Kiviranta, I., and Setton, L. A., 2000, "Simultaneous Changes in the Mechanical Properties, Quantitative Collagen Organization, and Proteoglycan Concentration of Articular Cartilage Following Canine Meniscectomy," J. Orthop. Res., **18**(3), pp. 383–392.

[10] Helminen, H. J., Saamanen, A. M., Salminen, H., and Hyttinen, M. M., 2002, "Transgenic Mouse Models for Studying the Role of Cartilage Macromolecules in Osteoarthritis," Rheumatology, **41**(8), pp. 848–856.

[11] Flahiff, C. M., Kraus, V. B., Huebner, J. L., and Setton, L. A., 2004, "Cartilage Mechanics in the Guinea Pig Model of Osteoarthritis Studied with an Osmotic Loading Method," Osteoarthritis Cartilage, **12**(5), pp. 383–388.

[12] Xu, L., Flahiff, C. M., Waldman, B. A., Wu, D., Olsen, B. R., Setton, L. A., and Li, Y., 2003, "Osteoarthritis-Like Changes and Decreased Mechanical Function of Articular Cartilage in the Joints of Mice with the Chondrodysplasia Gene (Cho)," Arthritis Rheum., **48**(9), pp. 2509–2518.

[13] Athanasiou, K. A., Zhu, C. F., Wang, X., and Agrawal, C. M., 2000, "Effects of Aging and Dietary Restriction on the Structural Integrity of Rat Articular Cartilage," Ann. Biomed. Eng., **28**(2), pp. 143–149.

[14] Hyttinen, M. M., Toyras, J., Lapvetelainen, J., Lindblom, J., Prockop, D. J., Li,

S.-W., Arita, M., Jurvelin, J. S., and Helminen, H. J., 2001, "Inactivation of One Allele of the Type II Collagen Gene Alters the Collagen Network in Murine Articular Cartilage and Makes Cartilage Softer," Ann. Rheum. Dis., **60**(3), pp. 262–268.
[15] Nelder, J. A., and Mead, R., 1965, "A Simplex Method for Function Minimization," Comput. J., **7**(4), pp. 308–313.
[16] Goldberg, D. E., 1989, *Genetic Algorithms in Search, Optimization and Machine Learning*, Kluwer Academic, Boston.
[17] Bulstra, S. K., Buurman, W. A., Walenkamp, G. H., and Van der Linden, A. J., 1989, "Metabolic Characteristics of In Vitro Cultured Human Chondrocytes in Relation to the Histopathologic Grade of Osteoarthritis," Clin. Orthop. Relat. Res., **242**, pp. 294–302.
[18] LeRoux, M. A., and Setton, L. A., 2002, "Experimental and Biphasic FEM Determinations of the Material Properties and Hydraulic Permeability of the Meniscus in Tension," J. Biomech. Eng., **124**(3), pp. 315–321.
[19] Mow, V. C., Kuei, S. C., Lai, W. M., and Armstrong, C. G., 1980, "Biphasic Creep and Stress Relaxation of Articular Cartilage in Compression: Theory and Experiment," J. Biomech. Eng., **102**(1), pp. 73–84.
[20] Storn, R., and Price, K., 1997, "Differential Evolution—A Simple and Efficient Heuristic for Global Optimization over Continuous Spaces," J. Global Optim., **11**, pp. 341–359.
[21] DiSilvestro, M. R., Zhu, Q., Wong, M., Jurvelin, J. S., and Suh, J. K., 2001, "Biphasic Poroviscoelastic Simulation of the Unconfined Compression of Articular Cartilage: I. Simultaneous Prediction of Reaction Force and Lateral Displacement," J. Biomech. Eng., **123**(2), pp. 191–197.
[22] Storn, R., and Price, K., 1996, "Minimizing the Real Functions of the ICEC'96 Contest by Differential Evolution," IEEE Conference on Evolutionary Computation, Nagoya, pp. 842–844.
[23] Brunschwig, A. S., and Salt, A. N., 1997, "Fixation-Induced Shrinkage of Reissner's Membrane and Its Potential Influence on the Assessment of Endolymph Volume," Hear. Res., **114**(1–2), pp. 62–68.
[24] Athanasiou, K. A., Rosenwasser, M. P., Buckwalter, J. A., Malinin, T. I., and Mow, V. C., 1991, "Interspecies Comparisons of In Situ Intrinsic Mechanical Properties of Distal Femoral Cartilage," J. Orthop. Res., **9**(3), pp. 330–340.
[25] Athanasiou, K. A., Agarwal, A., and Dzida, F. J., 1994, "Comparative Study of the Intrinsic Mechanical Properties of the Human Acetabular and Femoral Head Cartilage," J. Orthop. Res., **12**(3), pp. 340–349.
[26] Setton, L. A., Elliott, D. M., and Mow, V. C., 1999, "Altered Mechanics of Cartilage with Osteoarthritis: Human Osteoarthritis and an Experimental Model of Joint Degeneration," Osteoarthritis Cartilage, **7**(1), pp. 2–14.
[27] Leroux, M. A., Cheung, H. S., Bau, J. L., Wang, J. Y., Howell, D. S., and Setton, L. A., 2001, "Altered Mechanics and Histomorphometry of Canine Tibial Cartilage Following Joint Immobilization," Osteoarthritis Cartilage, **9**(7), pp. 633–640.
[28] Jurvelin, J. S., Buschmann, M. D., and Hunziker, E. B., 2003, "Mechanical Anisotropy of the Human Knee Articular Cartilage in Compression," Proc. Inst. Mech. Eng., Part H: J. Eng. Med., **217**(3), pp. 215–219.
[29] Mow, V. C., and Setton, L. A., 1998, "Mechanical Properties of Normal and Osteoarthritic Articular Cartilage," in *Osteoarthritis*, D. D. Brandt, M. Doherty, and L. S. Lohmander (eds.) Oxford University Press, New York, pp. 108–122.
[30] Soltz, M. A., and Ateshian, G. A., 2000, "A Conewise Linear Elasticity Mixture Model for the Analysis of Tension-Compression Nonlinearity in Articular Cartilage," J. Biomech. Eng., **122**(6), 576–586.